Research Article

Identification of potential oxidative stress biomarkers for spinal cord injury in erythrocytes using mass spectrometry

https://doi.org/10.4103/1673-5374.301487

Date of submission: May 7, 2020

Date of decision: July 3, 2020

Date of acceptance: August 20, 2020

Date of web publication: December 12, 2020

Li-Jian Zhang[1, 2, 3, #], Yao Chen[1, 2, 3, #], Lu-Xuan Wang[1], Xiao-Qing Zhuang[4, *], He-Chun Xia[2, 3, *]

Graphical Abstract *Erythrocyte can serve as a novel source of oxidative biomarkers for spinal cord injury*

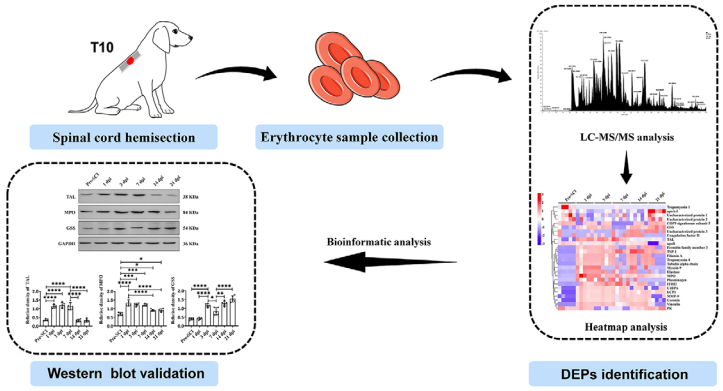

Abstract

Oxidative stress is a hallmark of secondary injury associated with spinal cord injury. Identifying stable and specific oxidative biomarkers is of important significance for studying spinal cord injury-associated secondary injury. Mature erythrocytes do not contain nuclei and mitochondria and cannot be transcribed and translated. Therefore, mature erythrocytes are highly sensitive to oxidative stress and may become a valuable biomarker. In the present study, we revealed the proteome dynamics of protein expression in erythrocytes of beagle dogs in the acute and subacute phases of spinal cord injury using mass spectrometry-based approaches. We found 26 proteins that were differentially expressed in the acute (0–3 days) and subacute (7–21 days) phases of spinal cord injury. Bioinformatics analysis revealed that these differentially expressed proteins were involved in glutathione metabolism, lipid metabolism, and pentose phosphate and other oxidative stress pathways. Western blot assays validated the differential expression of glutathione synthetase, transaldolase, and myeloperoxidase. This result was consistent with mass spectrometry results, suggesting that erythrocytes can be used as a novel sample source of biological markers of oxidative stress in spinal cord injury. Glutathione synthetase, transaldolase, and myeloperoxidase sourced from erythrocytes are potential biomarkers of oxidative stress after spinal cord injury. This study was approved by the Experimental Animal Centre of Ningxia Medical University, China (approval No. 2017-073) on February 13, 2017.

Key Words: acute phase; bioinformatic analysis; biomarkers; central nervous system; dog; erythrocytes; mass spectrometry; oxidative stress; peripheral blood; spinal cord injury; subacute phase

Chinese Library Classification No. R446; R741; R331.1+41

Introduction

Spinal cord injury (SCI) is a serious neurological deficit that affects both young and elderly populations worldwide, significantly reducing their quality of life (Anna et al., 2017; Motiei-Langroudi and Sadeghian, 2017; Badhiwala et al., 2019). The neurons and glial cells in the spinal cord are vulnerable to oxidative stress because of many factors, including their intense production of reactive oxygen metabolites, high rate of energy demand, and relatively low antioxidant capacity (Jia et al., 2012; Lassmann and van Horssen, 2016; Cheng et al., 2019). It has been suggested that oxidative stress plays significant roles in the pathophysiology

[1]School of Clinical Medicine, Ningxia Medical University, Yinchuan, Ningxia Hui Autonomous Region, China; [2]Department of Neurosurgery, General Hospital of Ningxia Medical University, Yinchuan, Ningxia Hui Autonomous Region, China; [3]Ningxia Human Stem Cell Research Institute, General Hospital of Ningxia Medical University, Yinchuan, Ningxia Hui Autonomous Region, China; [4]Department of Nuclear Medicine, General Hospital of Ningxia Medical University, Yinchuan, Ningxia Hui Autonomous Region, China

*Correspondence to: He-Chun Xia, MD, xhechun@nyfy.com.cn; Xiao-Qing Zhuang, PhD, zhuangxq@nyfy.com.cn.
https://orcid.org/0000-0002-3058-8162 (He-Chun Xia); https://orcid.org/0000-0001-8652-8540 (Xiao-Qing Zhuang); https://orcid.org/0000-0003-3881-7705 (Li-Jian Zhang); https://orcid.org/0000-0001-9071-2578 (Lu-Xuan Wang)
#Both authors contributed equally to this work.

Funding: *This work was supported by the Key Research Projects of the Ningxia Hui Autonomous Region of China, No. 2018BCG01002 (to HCX); and the Plan of Postgraduate Education Innovation, Discipline Construction Project of Ningxia, China (2017), No. YXW2017014 (to LJZ).*

How to cite this article: *Zhang LJ, Chen Y, Wang LX, Zhuang XQ, Xia HC (2021) Identification of potential oxidative stress biomarkers for spinal cord injury in erythrocytes using mass spectrometry. Neural Regen Res 16(7):1294-1301.*

of both acute and chronic SCI (Hall, 2011; Bastani et al., 2012; Fatima et al., 2015). Thus, alleviating oxidative stress might be an effective therapeutic approach for SCI treatment, and monitoring biomarkers of oxidative stress is important to assess pathogenic processes and guide therapeutic interventions for individuals with SCI (Bedreag et al., 2014).

Because of the complex nature of SCI, identification of the molecules involved in its pathogenesis is crucial. The emerging field of proteomics, with its objective to explore biomarker candidates and therapeutic targets, has received increasing attention in recent decades (Dunckley et al., 2005; Guest et al., 2013). In recent years, protein arrays and mass spectrometry (MS) have been used extensively to survey the oxidative stress biomarkers for SCI in spinal cord tissue and biofluids, and several putative biomarker candidates have been identified, including acrolein, glutathione (GSH), and malondialdehyde (Tully et al., 2014; Khoubnasabjafari et al., 2015; Yao et al., 2019; Xu et al., 2020). However, oxidative stress biomarkers are often short-lived, labile, and difficult to measure directly (Jansen et al., 2017). Thus, a novel source of oxidative stress biomarkers is still a pressing need.

Erythrocytes are critical components of peripheral blood. Because of their abundance and accessibility, erythrocytes have been suggested as potential targets for biomarkers of many diseases (Crawford et al., 2004). Evidence has indicated that erythrocytes lose all organelles when they mature, resulting in a lack of potential to replace proteins that have lost their functions, which makes them highly sensitive to any aberrations and especially prone to oxidative stress (Barasa and Slijper, 2014; Mazzulla et al., 2015). The exposure of erythrocytes to oxidative stress results in lipid peroxidation and alterations in cellular morphology and membrane protein conformation (Fujino et al., 2000; Okamoto et al., 2004). A previous study demonstrated increased lipid peroxidation with higher concentrations of thiobarbituric acid reactive substances in the erythrocytes of cervical SCI patients (Woźniak et al., 2016). Nightingale et al. (2020) examined the associations between erythrocyte distribution width and cardiorespiratory fitness in individuals with chronic SCI. Their data showed a positive correlation between the relative peak oxygen uptake and erythrocyte distribution width. Higher erythrocyte distribution width values are an independent risk factor for cardiovascular mortality, heart failure, and coronary heart disease and may reflect several underlying exacerbated metabolic responses such as oxidative stress (Nightingale et al., 2020). In addition, erythrocytes are also highly susceptible to oxidative damage because of their high concentrations of oxygen and hemoglobin. These properties make erythrocytes a suitable model to investigate oxidative damage (Pandey and Rizvi, 2011; Tsakanova et al., 2017; Revin et al., 2019). Recent studies reported erythrocytes as a valuable biomarker in the clinical management of oxidative stress-associated diseases, such as chronic obstructive pulmonary disease and primary open-angle glaucoma (Lucantoni et al., 2006; Rokicki et al., 2016). Despite their potential, erythrocytes have not yet been examined to select oxidative stress biomarkers for SCI.

Dogs have not only heterogeneity of both injury and genetic backgrounds but also histopathological similarities to human patients, which could closely mirror the pathogenesis of humans (Jeffery et al., 2005; Dalgaard, 2015). Moreover, dogs with SCI represent a large animal model that offers unique benefits for SCI research, which could bridge the large gap between human and rodent studies (Bock et al., 2013; Moore et al., 2017). For the first time, we analyzed the proteomic profiles of erythrocytes in the acute and subacute phases of SCI in a dog model using MS.

Materials and Methods

Animals

Five male beagle dogs (aged 12–24 months; weight 13–17 kg) were provided by the Experimental Animal Centre of Ningxia Medical University, China (License No. 2017-073). The dogs were housed under standard conditions (temperature: 21–25°C; humidity: 30–40%; 12-hour light/dark cycle) with standard dog chow twice daily and water available *ad libitum*. All surgical procedures were approved by the Experimental Animal Centre of Ningxia Medical University, China (approval No. 2017-073) on February 13, 2017.

SCI model

Analgesics (2.5 mg/kg; tramadol hydrochloride, CSPC Pharmaceutical Co., Ltd., Shijiazhuang, China; intramuscularly injected into the thigh muscle of the right femur) were given to the dogs 30 minutes before the operation. The animals were anesthetized with dexmedetomidine (10 μg/kg; Dexdomitor; Orion Corporation, Espoo, Finland; intramuscularly injected into the thigh muscle of the right femur) and then maintained under spontaneous ventilation with 2.0–3.0% isoflurane in oxygen. During the operation, the body temperature of the dogs was maintained with a heating pad. The surgical areas were shaved and prepared with iodophors. Using sanitized instruments, laminectomy was performed at the tenth thoracic segment (T10), and then unilateral (left side) hemisection at the T10 level was performed with micro-scissors (Zhang et al., 2020). After the operation, manual bladder expression was performed at least three times per day until voluntary urination was established. The general condition of the dogs and their neurological status was monitored twice daily during the study period, and no complications occurred (Ryu et al., 2009).

Erythrocyte sample preparation and lysis and membrane protein extraction

Blood samples (5 mL) were obtained with a 24-G intravenous catheter (Becton Dickinson Ltd., Oxford, UK) from the jugular vein of each dog in the acute phase (0, 1, and 3 days post-injury (dpi)) and subacute phase (7, 14, and 21 dpi) (Moore et al., 2017). All samples and buffers were kept at 4°C during all steps. Erythrocytes were separated by centrifugation for 5 minutes at 2000 × *g* and resuspended in Lymphocyte H (Cedarlane, Burlington, ON, USA) with centrifugation as described. Then, erythrocytes were washed three times in 5 mM phosphate buffer (pH 8.0) containing 0.9% (w/v) NaCl and then centrifuged at 30,000 × *g* for 10 minutes at 4°C. The remaining erythrocyte fraction was passed through nylon filters to further eliminate granulocytes, washed three times in 5 mM phosphate buffer (pH 8.0) containing 0.9% (w/v) NaCl, and then centrifuged at 30,000 × *g* for 10 minutes at 4°C. The remaining erythrocytes were immediately used to extract membrane and lysis proteins, as previously described (Pasini et al., 2006; Pallotta et al., 2015).

Liquid chromatography-tandem MS analysis

Analysis of the peptide mixtures was performed using a Q Exactive HF mass spectrometer (Thermo Fisher Scientific, Palo Alto, CA, USA) (Scheltema et al., 2014). Aliquots of 5 μg of total peptide were subjected to chromatography on a 50-cm column with a 75-μm inner diameter packed with C18 material. Peptide separation was carried out at 300 nL/min for 75 minutes using a two-step acetonitrile gradient of 5–40% over the first 60 minutes and 40–95% for the following 15 minutes. The back pressure varied between 450 and 650 bar (1 bar = 100 kPa). The temperature of the column oven was 55°C. The mass spectrometer was operated in data-dependent mode with survey scans acquired at a resolution of 50,000 at a mass-to-charge ratio (m/z) of 400 (transient time 256 ms). Up to 15 of the most abundant isotope patterns with charges ≥ +2 from the survey scan (300–1650 m/z)

were selected with an isolation window of 1.6 m/z and were fragmented by high-energy collisional dissociation with a normalized collision energy of 25. The maximum ion injection times for the survey scan and the tandem MS scans were 20 and 60 ms, respectively. The ion target values for the MS1 and MS2 scan modes were set to 3×10^6 and 3×10^5, respectively. The dynamic exclusion was 25 seconds and 10 ppm (Michalski et al., 2011; Bryk and Wiśniewski, 2017).

Bioinformatic analysis of differentially expressed proteins

The log2 transformed data of differentially expressed proteins (DEPs) were visualized by heatmaps with the R software package gplots, version 3.0.1 (https://www.r-project.org/). A principal component analysis (PCA) model was visualized for the clustering trend based on the variation in phase of injury using the 'principal' function in R software (Parent et al., 2016). Gene Ontology and Kyoto Encyclopedia of Genes and Genomes analyses were performed with the Database for Annotation, Visualization and Integrated Discovery (http://david.abcc.ncifcrf.gov/), and the protein-protein interaction network was mapped using STRING v 9.1 (http://string91.embl.de/) (Franceschini et al., 2013).

Validation of representative protein expression levels by western blot analysis

To validate the expression changes of representative proteins involved in oxidative-related pathways, myeloperoxidase (MPO), transaldolase (TAL), and GSH synthetase (GSS) expression levels were detected by western blot assays, with glyceraldehyde 3-phosphate dehydrogenase as a control. Briefly, 25 μg of each protein from the erythrocyte sample extracts was resolved by sodium dodecyl sulfate-polyacrylamide gel electrophoresis on a 4–12% Bis-Tris Criterion XT Precast Gel (Bio-Rad Laboratories, Solna, Sweden) according to the manufacturer's instructions. The proteins were transferred onto a nitrocellulose membrane (Invitrogen, Carlsbad, CA, USA), and the blot was blocked for 1 hour at room temperature. The membrane was then washed briefly with 50 mM Tris-buffered saline and 0.5% Tween-20 (pH 8.0) twice prior to incubation with primary antibodies in 0.5% fat-free milk in 50 mM Tris-buffered saline and 0.5% Tween-20 (pH 8.0) overnight at 4°C under gentle agitation. The following primary antibodies were diluted as indicated and used for immunoblotting: rabbit anti-TAL (Cat# ab187689; 1:500; Abcam, Cambridge, UK), mouse anti-MPO (Cat# MCA1757, 1:1000, Bio-Rad, Hercules, CA, USA), mouse anti-GSS (Cat# ABIN1498538, 1:200, Antibodies-Online Inc., Atlanta, GA, USA), and rabbit anti-glyceraldehyde 3-phosphate dehydrogenase (Cat# ab9485; 1:2500; Abcam). The membranes were washed three times for 10 minutes each with Tris-buffered saline and then incubated with goat-anti-mouse horseradish peroxidase-conjugated IgG (Cat# sc-2004, 1:5000, Santa Cruz Biotechnology, Santa Cruz, CA, USA) for 90 minutes at room temperature. After the membranes were again washed three times with Tris-buffered saline, the immunoreactive bands were detected with an enhanced chemiluminescence detection kit (Amersham Biosciences GE, Little Chalfont, UK) and imaged with a ChemiDoc XRS+ system (Bio-Rad). Equal protein loading was verified by Ponceau red staining of the membranes (Abu Hamdeh et al., 2018).

Statistical analysis

All statistical analysis was performed with GraphPad Prism 7.0 (GraphPad Software, La Jolla, CA, USA). Repeated measures analysis of variance followed by Dunnett's *post hoc* test was used for statistical analysis. All values are expressed as the mean ± standard deviation (SD). A value of $P < 0.05$ was considered to indicate a statistically significant difference. Protein identification from the MS data was accomplished using Proteome Discoverer software (version 1.4.0.288; Thermo Fisher Scientific). We referred to the latest UniProt data, Uniprot-SwissProt (Taxonomy: Canis lupus familiaris, 25 493 entries), to identify the proteins using Mascot (version 2.3.2; Matrix Science). Peptide scores were assigned and the false discovery rate was estimated using the Percolator algorithm to control the false positive rate. The main parameters are as follows: minimum (min) peptide length: 6 amino acids; maximum (max) peptide length: 144 amino acids; min precursor mass: 350 Da; max precursor mass: 5000 Da; precursor mass tolerance: 10 ppm; fragment mass tolerance: 0.05 Da; variable modification: oxidation (M), acetyl (protein N-term). Proteins with a P value < 0.05 or with a false discovery rate < 0.05 were identified as significantly DEPs.

Results

Protein profiling in erythrocytes in a dog model of SCI

Erythrocyte protein extracts obtained pre-SCI and at 1, 3, 7, 14, and 21 dpi were subjected to combined liquid chromatography-tandem MS analysis. In total, 319 proteins were identified. We identified 26 DEPs at different time points after SCI (**Figure 1**). Among the DEPs, we found that three uncharacterized proteins were significantly dysregulated after SCI (**Table 1**). To investigate the temporal expression patterns of those DEPs after SCI, a heatmap analysis was performed (**Figure 1**). As shown in **Figure 2**, the level of TAL was significantly increased within 7 dpi, with expression levels peaking at 3 dpi ($P = 0.0005$, $n = 5$). At 14 and 21 dpi, the TAL level was significantly decreased compared with that pre-SCI ($P = 0.0180$, $n = 5$; $P = 0.0028$, $n = 5$, respectively). The MPO level tended to be upregulated at all stages compared with that pre-SCI, and the peak of its expression was observed at 1 dpi ($P < 0.0001$, $n = 5$). During the acute and subacute stages of SCI, the change in the GSS level occurred in a biphasic manner. The GSS level was significantly increased at 3 dpi compared with that pre-SCI ($P = 0.0002$, $n = 5$). After a significant decrease at 7 dpi, the GSS level was significantly increased at 14 and 21 dpi ($P < 0.0001$, $n = 5$; $P < 0.0001$, $n = 5$, respectively). Compared with the pre-SCI level, the expression of pyruvate kinase (PK) was significantly decreased at 1, 3, 7, and 14 dpi ($P = 0.0004$, $n = 5$; $P < 0.0001$, $n = 5$; $P < 0.0001$, $n = 5$; $P = 0.0003$, $n = 5$, respectively). Then, the PK level increased to the pre-SCI level at 21 dpi ($P = 0.9995$, $n = 5$). The apolipoprotein (apo) A-I level tended to decrease at 1 dpi, but without a significant difference compared with that pre-SCI, and then increased markedly at 21 dpi ($P = 0.0831$, $n = 5$; $P = 0.0001$, $n = 5$, respectively).

PCA of erythrocyte proteins

Next, PCA of erythrocyte proteins from the 1 dpi and pre-SCI samples was performed to investigate the variance in these data (**Figure 3A**). The first principal component (PC1) accounted for 55.9% of the total variance among samples from pre-SCI dogs and SCI dogs. Changes in inter-alpha-trypsin inhibitor heavy chain 2, vinculin, and thrombospondin 1 contributed to this separation between groups. The second principal component (PC2) accounted for an additional 18.0% of the total variance among samples from SCI dogs and pre-SCI dogs. Changes in MPO and PK contributed to this separation between groups. All of these proteins are involved in neuroinflammation, actin binding, cell-extracellular matrix adhesion, and carbohydrate metabolism.

PCA of erythrocyte samples at 1, 3, 7, 14, and 21 dpi also demonstrated differences in protein expression patterns over time. In our second PCA model, 32.1% of the variance was explained by PC1, and 15.8% was explained by PC2. As shown in **Figure 3B**, there were indications of clustering, with more pronounced separation of the proteins expressed on 21 dpi. Elastase, tubulin alpha chain, TAL, GSS, apoA-I, and constitutive photomorphogenesis 9 signalosome subunit 5 contributed to this separation. All of these proteins are associated with oxidative stress, inflammatory responses, and

Table 1 | Differentially expressed proteins identified by liquid chromatography-tandem mass spectrometry analysis in erythrocytes following spinal cord injury

Uniprot ID	Protein description	FDR	*P*-value
F1P916	Tropomyosin 1	0.0346	0.0001
F1PDJ5	Apolipoprotein A-I	0.1716	0.0039
F1PSX2	Uncharacterized protein 1	0.4847	0.0349
L7N0F2	Uncharacterized protein 2	0.3008	0.0131
E2QWE0	Constitutive photomorphogenesis 9 signalosome subunit 5	0.1715	0.0034
F1Q2D2	Glutathione synthetase	0.4697	0.0279
F1Q0J0	Uncharacterized protein 3	0.2733	0.0103
E2RRM2	Coagulation factor II, thrombin	0.5211	0.0417
H9GW87	Transaldolase	0.4697	0.0261
F1P8Z5	Apolipoprotein B	0.4697	0.0303
E2RK64	Fermitin family member 3	0.4697	0.0294
F1PBI6	Thrombospondin 1	0.2323	0.0080
F1PWW0	Filamin A	0.1879	0.0053
F6X7L0	Tropomyosin 4	0.4697	0.0309
L7N0G4	Tubulin alpha chain	0.3008	0.0135
F1P9J3	Myosin-9	0.5212	0.0406
Q8MJD1	Elastase	0.3008	0.0141
J9P0R6	Myeloperoxidase	0.5212	0.0424
F1Q421	Plasminogen	0.4778	0.0329
F1PG39	Inter-alpha-trypsin inhibitor heavy chain 2	0.2323	0.0073
F1PGM9	Complement component 4 binding protein alpha	0.4331	0.0217
E2QWN7	Lymphocyte cytosolic protein 1	0.1716	0.0043
F1P6A2	Matrix metalloproteinase-9	0.0618	0.0008
E2QSZ5	Coronin	0.0835	0.0013
J9P4F3	Vinculin	0.0345	0.0003
F1PHR2	Pyruvate kinase	0.0345	0.0003

Differentially expressed proteins were selected based on a *P*-value < 0.05 or FDR < 0.05. FDR: False discovery rate.

cytoplasmic translocation.

Bioinformatic analysis of DEPs

To identify the biological function represented by the DEPs, Gene Ontology analysis and Kyoto Encyclopedia of Genes and Genomes pathway enrichment analysis were performed. As shown in **Figure 4** and **Additional Table 1**, the results of Gene Ontology annotation enrichment indicated that the most significantly enriched biological process terms for the DEPs post injury were cell migration, cell motility, and movement of cell or subcellular component. The most significantly enriched molecular function terms for the DEPs post-injury were lipoprotein particle, protein-lipid complex binding, and sulfur compound terms. The most noteworthy enriched cellular component terms of the DEPs post-injury were cytoplasmic vesicle, intracellular vesicle, and phagocytic vesicle terms.

The results of Kyoto Encyclopedia of Genes and Genomes pathway enrichment analysis of the 26 overlapping DEPs are shown in **Additional Table 2**. The Kyoto Encyclopedia of Genes and Genomes pathways were mainly enriched in oxidative stress-related pathways, such as the phagosome, GSH metabolism, lipid metabolism, and pentose phosphate pathways.

Protein-protein interaction prediction was performed with STRING software. As shown in **Figure 5**, the proteins thrombospondin 1, matrix metallopeptidase 9, inter-alpha-trypsin inhibitor heavy chain 2, and tropomyosin 4 were located in the most central area of the network. Plasminogen, MPO, myosin-9, apoA-I, apoB, and tropomyosin-1 were located in the outermost part of the network, and GSS and PK were not included in the network.

Validation of representative protein expression levels by western blot analysis

From the list of DEPs, we selected three representative proteins involved in key pathways for western blot validation (**Figure 6A**). Our results showed significant alteration in MPO, TAL, and GSS expression post-injury. The expression level of MPO was significantly upregulated after SCI and peaked at 1 dpi ($P < 0.0001$, $n = 5$). The TAL level was significantly increased at 1, 3, and 7 dpi ($P = 0.0218$, $n = 5$; $P = 0.0035$, $n = 5$; $P = 0.0177$, $n = 5$, respectively) and then decreased to the baseline level at 14 and 21 dpi. The expression of GSS exhibited a biphasic pattern. The GSS level initially increased sharply at 3 dpi compared with the pre-SCI level ($P = 0.0048$, $n = 5$). After a significant decrease at 7 dpi, the GSS level was significantly increased at 14 and 21 dpi ($P = 0.0003$, $n = 5$; $P < 0.0001$, $n = 5$, respectively) (**Figure 6B**). The results were consistent with the observations in the proteomic analysis.

Discussion

It has been reported that increased generation of reactive oxygen species and consequent oxidative stress are important events associated with SCI (Xu et al., 2005; Jia et al., 2012; Fatima et al., 2015; Visavadiya et al., 2016; Rios et al., 2018). Despite its postulated roles in the progression of SCI, there is only limited information on the oxidation status following SCI. In an effort to acquire a better understanding of oxidative stress-related pathologies and to identify novel potential sources of oxidative stress biomarkers, we investigated the proteomic profiles of erythrocytes in dogs in the acute and subacute phases of SCI. Using MS-based proteomics approaches, we identified a panel of antioxidant and oxidative stress biomarkers in erythrocytes. Our results suggested that erythrocytes might be a potential source of oxidation biomarkers and therapeutic target discovery.

With the development of high-throughput techniques for biomarker discovery, the field of oxidative stress biomarkers has rapidly expanded (Donato et al., 2020a, b). In this study, we identified several DEPs involved in GSH metabolism, lipid metabolism, and pentose phosphate pathways, including GSS, TAL, and MPO. These oxidation pathways and their reducing reactions were involved in different phases of SCI. MPO, as a pro-oxidant enzyme, exacerbates secondary injury of SCI not only by generating the strong oxidant hypochlorous acid, but also by enhancing neutrophil infiltration into the injury site (Fleming et al., 2006; Yap et al., 2006; Kubota et al., 2012). In our study, we found that MPO expression was significantly upregulated in the acute phase of SCI and peaked at 1 dpi. In contrast to our observation, a previous study using a dog model revealed that MPO levels in both plasma and cerebrospinal fluid significantly increased at 4 hours after SCI and then sharply decreased within 3 days (Awad et al., 2008). The reason for this time difference is not clear but may result from the use of different types of injury models. Typically, MPO is abundantly expressed in immune cells, including microglia, monocytes, and astrocytes (Lefkowitz and Lefkowitz, 2008; Tavora et al., 2009; Odobasic et al., 2016). In addition, circulating MPO binds rapidly to erythrocyte membranes through electrostatic interactions, and an increased MPO concentration in erythrocytes coincides with higher MPO plasma levels (Adam et al., 2014; Gorudko et al., 2016). MPO is a known prognostic biomarker for inflammatory neurodegenerative diseases, including SCI (Forghani et al., 2012; Albadawi et al., 2017). Our PCA results indicated that MPO can also contribute to distinguishing between SCI dogs and pre-SCI dogs. Therefore, considering our observations, we proposed that MPO in erythrocytes might be of clinical relevance as well.

As an antioxidant defense, the pentose phosphate pathway and GSH metabolism pathway are involved in both the acute

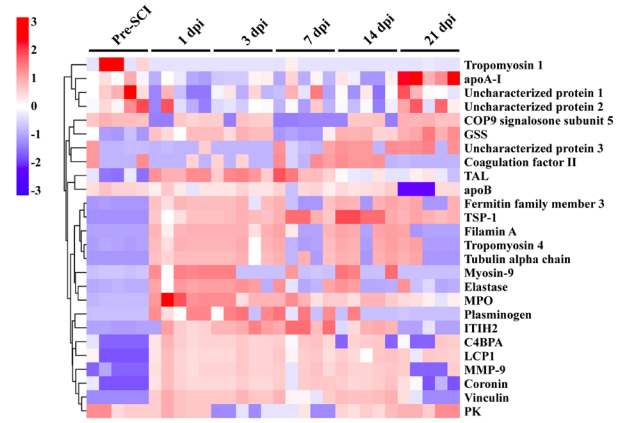

Figure 1 | Heatmap and hierarchical cluster analysis of the DEPs after SCI.
The heatmap illustrates the dynamic changes in the expression levels of DEPs. Each time point includes five samples. The values are the z-scores of the normalized protein expression levels. The color bar in the heatmap ranges from dark blue, indicating low expression, to dark red, indicating high expression. DEPs: Differentially expressed proteins; dpi: day(s) post-injury; SCI: spinal cord injury.

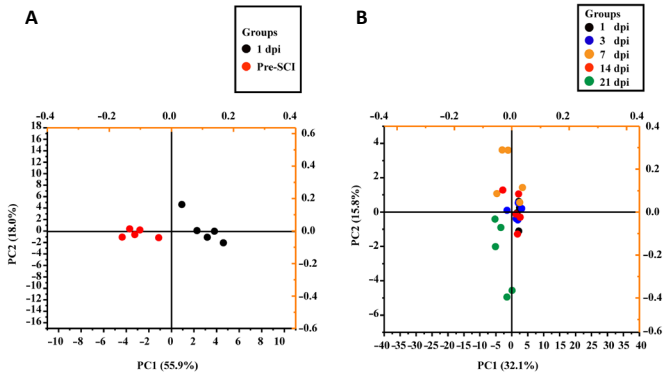

Figure 3 | Principal component analysis of protein expression in erythrocytes of SCI dogs.
(A) The variance in protein expression between pre-SCI and 1 dpi. (B) The variance in protein expression at 1, 3, 7, 14, and 21 dpi. dpi: Day(s) post-injury; PC1: first principal component; PC2: second principal component; SCI: spinal cord injury.

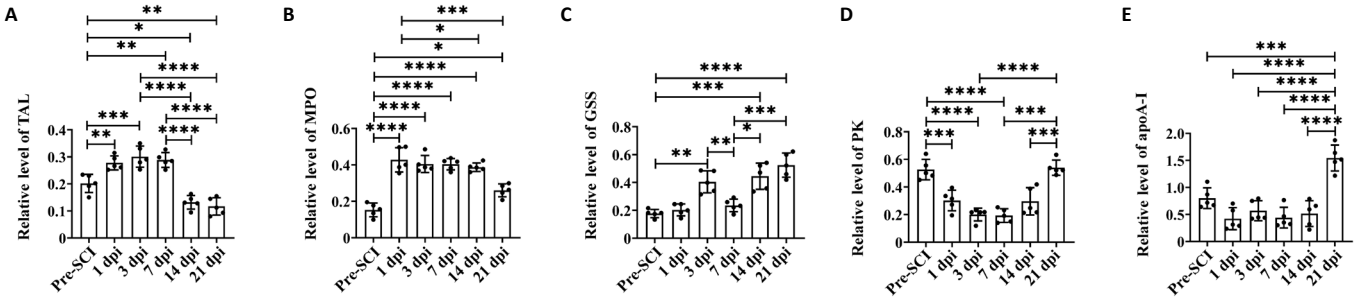

Figure 2 | Relative level of TAL, MPO, GSS, PK, and apoA-I in erythrocytes of SCI dogs.
(A) TAL, (B) MPO, (C) GSS, (D) PK, and (E) apoA-I were differentially expressed proteins detected by liquid chromatography-tandem mass spectrometry analysis. Data are expressed as the mean ± SD (n = 5). *P < 0.05, **P < 0.01, ***P < 0.001, ****P < 0.0001 (repeated measures analysis of variance followed by Dunnett's *post hoc* test). apoA-I: Apolipoprotein A-I; dpi: day(s) post-injury; GSS: glutathione synthetase; MPO: myeloperoxidase; PK: pyruvate kinase; SCI: spinal cord injury; TAL: transaldolase.

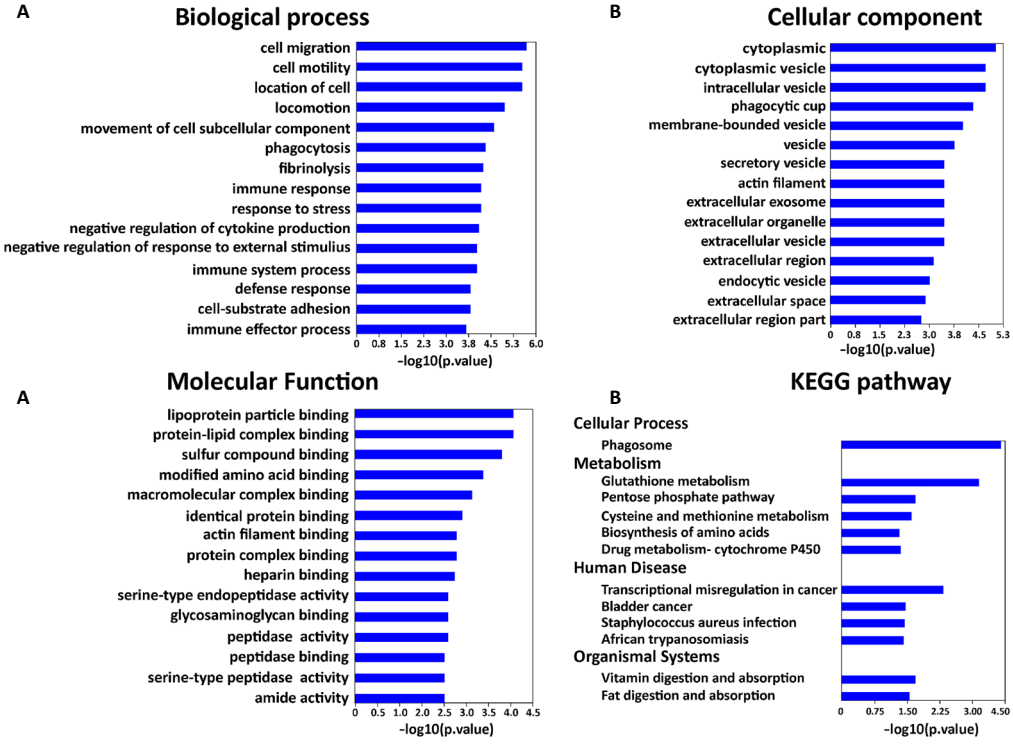

Figure 4 | GO enrichment and KEGG pathway analysis of differentially expressed proteins in erythrocytes of spinal cord injury dogs according to biological processes.
(A–C) The top 15 GO categories of biological process (A), cellular component (B), and molecular function (C). (D) KEGG pathway analysis of the differentially expressed proteins. GO: Gene Ontology; KEGG: Kyoto Encyclopedia of Genes and Genomes.

and subacute phases of SCI. GSH and enzymes are essential components for detoxification of reactive oxygen species as well as for the reduction and repair of oxidative cellular damage. In this study, we found that the GSS level was significantly upregulated in the acute phase (within 3 dpi) of SCI. Many studies have reported that dysregulation of GSS expression might be associated with various pathological processes associated with neurological diseases, including SCI (Sharma et al., 2004; Hayes et al., 2005; Kumar et al., 2017). One of the major roles of GSS is participation in the synthesis of GSH, which can protect cells not only against reactive oxygen species but also against their toxic products. Additionally, promotion of GSH synthesis could decrease reactive oxygen species and thereby attenuate secondary damage following SCI (Kamencic et al., 2001; Dash et al., 2016). Moreover, GSH is a crucial cofactor of the glyoxalase system. Evidence has indicated that the activity of glyoxalase 1, a detoxification enzyme, is highly dependent on adequate GSH levels (Donato et al., 2018). Moreover, glyoxalase 1 has been reported to be linked to neurodegenerative disease and oxidative stress-related pathologies, such as retinitis pigmentosa and cerebral cavernous malformations (Rinaldi et al., 2015; Donato et al., 2020c). Thus, we hypothesized that glyoxalase 1 might serve as a potential therapeutic target for oxidation-reduction following SCI, which deserves further investigation in future work. Our data showed that the TAL level was significantly decreased in the subacute phase of SCI. Previous studies have demonstrated that the pentose phosphate pathway controls oxidative stress via nicotinamide adenine dinucleotide phosphate (NADPH) production, which can protect against oxidation directly by neutralizing reactive oxygen intermediates or indirectly by regenerating GSH (Meloni et al., 2008; Perl et al., 2011). TAL is a key rate-limiting enzyme in the control of the nonoxidative branch of the pentose phosphate pathway and is responsible for the generation of NADPH to maintain GSH in a non-oxidized state. Suppression of TAL activity augments GSH levels and inhibits apoptosis by reducing oxidative stress (Banki et al., 1996). We proposed that the decrease of TAL and the increase of GSS might participate in antioxidant processes in the subacute phase of SCI. As a glycolytic enzyme, PK expression was inhibited in the acute phase of SCI, possibly because of the disruption of GSH homeostasis by oxidative modification. A decrease of PK leads to a decline in cellular ATP content, which affects the redox homeostasis (Tang et al., 2015). In this study, we also found a significant increase in PK activity that began at 14 dpi. Considering the changes in GSS and TAL activity, we proposed that PK is reactivated by the GSH-dependent redox system in the acute phase of SCI (Ogasawara et al., 2008).

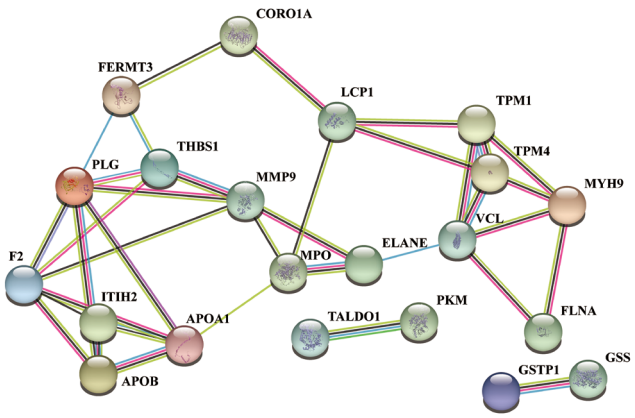

Figure 5 | **The protein-protein interaction of differentially expressed proteins in erythrocytes of spinal cord injury dogs.**
Pink lines indicate the presence of fusion evidence; green lines indicate neighborhood evidence; blue lines indicate co-occurrence evidence; yellow lines indicate text-mining evidence; light blue lines indicate database evidence; purple lines indicate experimental evidence; and black lines indicate co-expression evidence.

Moreover, a significant upregulation of lipid metabolism was observed in the subacute phase of SCI. With regard to long-term SCI, previous studies have documented that SCI patients have a high prevalence of lipid disorders (Myers et al., 2007; Phillips and Krassioukov, 2015). In this study, we found that apoA-I expression was significantly increased at 21 dpi. Current evidence suggests that apoA-I is a multifunctional apo that plays various roles in neurodegenerative disorders through its antioxidant and anti-inflammatory properties (Keeney et al., 2013). A study claimed that apoA-I might be of greatest diagnostic value in individuals with lipid abnormalities (Walldius et al., 2001). Nevertheless, our results are not consistent with those of published studies. Ozgurtas et al. (2003) characterized the serum lipid profiles of SCI patients, and their data showed reduced levels of high-density lipoprotein cholesterol and apoA-I in these patients compared with control subjects. Further work is needed to address such discrepancies. Our PCA results demonstrated that apoA-I contributed to distinguishing the 21 dpi samples from those at other time points. The expression of apoA-I in erythrocytes might serve as a potential biomarker of subacute oxidative stress. We proposed that the expression changes in apoA-I in erythrocytes make apoA-I a potential biomarker candidate for SCI and could provide insight for a better understanding of its mechanisms. However, this study has limitations. Because of the small sample size, a larger cohort study should be conducted to validate our results in the future. Moreover, this study is only focused on the acute and subacute stages of SCI. It is also very important to investigate alterations in the expression levels of DEPs in the chronic phase of SCI.

In conclusion, the current study is the first to explore erythrocytes as a potential source of oxidative biomarkers

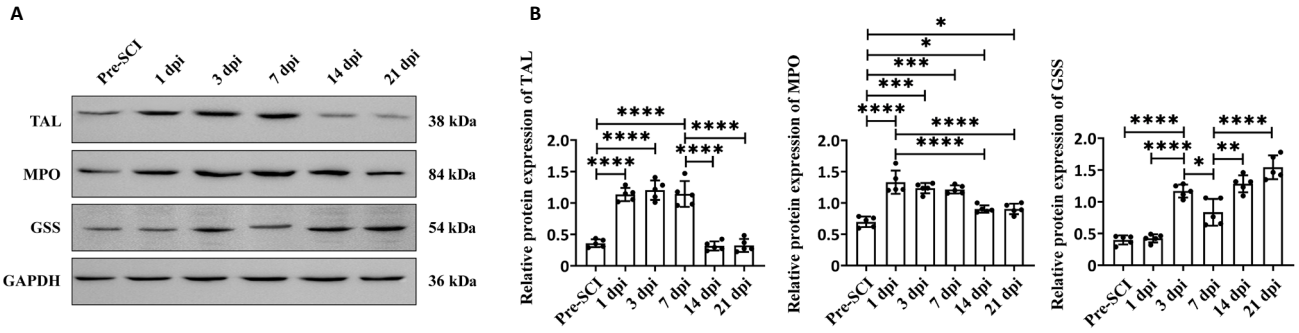

Figure 6 | **Western blot analysis of protein expression of TAL, MPO, and GSS in erythrocytes of dogs following SCI.**
(A) Representative blots for each protein. The band intensities were assessed by scanning densitometry. (B) The relative protein expression (optical density ratio to GAPDH) of the representative proteins TAL, MPO, and GSS. Data are expressed as the mean ± SD (n = 5). *P < 0.05, **P < 0.01, ***P < 0.001, ****P < 0.0001 (repeated measures analysis of variance followed by Dunnett's *post hoc* test). dpi: Day(s) post-injury; GAPDH: glyceraldehyde 3-phosphate dehydrogenase; GSS: glutathione synthetase; MPO: myeloperoxidase; SCI: spinal cord injury; TAL: transaldolase.

for SCI. Our study characterized the dynamic changes in protein expression in erythrocytes in the acute and subacute phases of SCI and provided a panel of potential oxidative stress biomarkers for SCI that hold promise as therapeutic targets and potential biomarkers. The data presented here may further our understanding of the molecular mechanisms underlying the development and progression of oxidative stress following SCI.

Author contributions: *Study conception and design: HCX, XQZ, LJZ; data analysis and manuscript drafting: XQZ, LJZ; experiment implementation and data collection: LJZ, YC, LXW; manuscript preparation: LJZ, XQZ; manuscript editing: HCX, XQZ. All authors approved the final version of the manuscript.*
Conflicts of interest: *The authors declare that they have no conflict of interest.*
Financial support: *This work was supported by the Key Research Projects of the Ningxia Hui Autonomous Region of China, No. 2018BCG01002 (to HCX); and the Plan of Postgraduate Education Innovation, Discipline Construction Project of Ningxia, China (2017), No. YXW2017014 (to LJZ). The funding sources had no role in study conception and design, data analysis or interpretation, paper writing or deciding to submit this paper for publication.*
Institutional review board statement: *The study was approved by the Experimental Animal Centre of Ningxia Medical University (approval No. 2017-073) on February 13, 2017.*

Data sharing statement: *Datasets analyzed during the current study are available from the corresponding author on reasonable request.*
Plagiarism check: *Checked twice by iThenticate.*
Peer review: *Externally peer reviewed.*

Open peer reviewers: *Jae Kyu Ryu, Gladstone Institute of Neurological disease, USA; William Rodemer, University of Pennsylvania, USA.*
Additional files:
Additional Table 1: *Gene ontology (GO) functional enrichment analysis for the differentially expressed proteins in erythrocytes of dogs following spinal cord injury.*
Additional Table 2: *Pathway enrichment analysis for the differentially expressed proteins in erythrocytes following spinal cord injury.*
Additional file 1: *Open peer review reports 1 and 2.*

References

Abu Hamdeh S, Shevchenko G, Mi J, Musunuri S, Bergquist J, Marklund N (2018) Proteomic differences between focal and diffuse traumatic brain injury in human brain tissue. Sci Rep 8:6807.
Adam M, Gajdova S, Kolarova H, Kubala L, Lau D, Geisler A, Ravekes T, Rudolph V, Tsao PS, Blankenberg S, Baldus S, Klinke A (2014) Red blood cells serve as intravascular carriers of myeloperoxidase. J Mol Cell Cardiol 74:353-363.
Albadawi H, Chen JW, Oklu R, Wu Y, Wojtkiewicz G, Pulli B, Milner JD, Cambria RP, Watkins MT (2017) Spinal cord inflammation: molecular imaging after thoracic aortic ischemia reperfusion injury. Radiology 282:202-211.
Anna Z, Katarzyna JW, Joanna C, Barczewska M, Joanna W, Wojciech M (2017) Therapeutic potential of olfactory ensheathing cells and mesenchymal stem cells in spinal cord injuries. Stem Cells Int 2017:3978595.
Awad H, Suntres Z, Heijmans J, Smeak D, Bergdall-Costell V, Christofi FL, Magro C, Oglesbee M (2008) Intracellular and extracellular expression of the major inducible 70kDa heat shock protein in experimental ischemia-reperfusion injury of the spinal cord. Exp Neurol 212:275-284.
Badhiwala JH, Wilson JR, Fehlings MG (2019) Global burden of traumatic brain and spinal cord injury. Lancet Neurol 18:24-25.
Banki K, Hutter E, Colombo E, Gonchoroff NJ, Perl A (1996) Glutathione levels and sensitivity to apoptosis are regulated by changes in transaldolase expression. J Biol Chem 271:32994-33001.
Barasa B, Slijper M (2014) Challenges for red blood cell biomarker discovery through proteomics. Biochim Biophys Acta 1844:1003-1010.
Bastani NE, Kostovski E, Sakhi AK, Karlsen A, Carlsen MH, Hjeltnes N, Blomhoff R, Iversen PO (2012) Reduced antioxidant defense and increased oxidative stress in spinal cord injured patients. Arch Phys Med Rehabil 93:2223-2228. e2.
Bedreag OH, Rogobete AF, Sărăndan M, Cradigati A, Păpurică M, Roşu OM, Dumbuleu CM, Săndesc D (2014) Oxidative stress and antioxidant therapy in traumatic spinal cord injuries. Rom J Anaesth Intensive Care 21:123-129.
Bock P, Spitzbarth I, Haist V, Stein VM, Tipold A, Puff C, Beineke A, Baumgärtner W (2013) Spatio-temporal development of axonopathy in canine intervertebral disc disease as a translational large animal model for nonexperimental spinal cord injury. Brain Pathol 23:82-99.
Bryk AH, Wiśniewski JR (2017) Quantitative analysis of human red blood cell proteome. J Proteome Res 16:2752-2761.
Cheng JP, Li H, Li XJ (2019) Extract of piper auritum can alleviate oxidative stress and inflammation of rat models of acute spinal cord injury. Zhongguo Zuzhi Gongcheng Yanjiu 23:5010-5016.
Crawford JH, Chacko BK, Kevil CG, Patel RP (2004) The red blood cell and vascular function in health and disease. Antioxid Redox Signal 6:992-999.
Dalgaard L (2015) Comparison of minipig, dog, monkey and human drug metabolism and disposition. J Pharmacol Toxicol Methods 74:80-92.
Dash PK, Hergenroeder GW, Jeter CB, Choi HA, Kobori N, Moore AN (2016) Traumatic brain injury alters methionine metabolism: implications for pathophysiology. Front Syst Neurosci 10:36.
Donato L, D'Angelo R, Alibrandi S, Rinaldi C, Sidoti A, Scimone C (2020a) Effects of A2E-induced oxidative stress on retinal epithelial cells: new insights on differential gene response and retinal dystrophies. Antioxidants (Basel) 9:307.
Donato L, Scimone C, Alibrandi S, Rinaldi C, Sidoti A, D'Angelo R (2020b) Transcriptome analyses of lncRNAs in A2E-stressed retinal epithelial cells unveil advanced links between metabolic impairments related to oxidative stress and retinitis pigmentosa. Antioxidants (Basel) 9:318.
Donato L, Scimone C, Nicocia G, Denaro L, Robledo R, Sidoti A, D'Angelo R (2018) GLO1 gene polymorphisms and their association with retinitis pigmentosa: a case-control study in a Sicilian population. Mol Biol Rep 45:1349-1355.
Donato L, Scimone C, Alibrandi S, Nicocia G, Rinaldi C, Sidoti A, D'Angelo R (2020c) Discovery of GLO1 new related genes and pathways by RNA-Seq on A2E-stressed retinal epithelial cells could improve knowledge on retinitis pigmentosa. Antioxidants (Basel) 9:416.
Dunckley T, Coon KD, Stephan DA (2005) Discovery and development of biomarkers of neurological disease. Drug Discov Today 10:326-334.
Fatima G, Sharma VP, Das SK, Mahdi AA (2015) Oxidative stress and antioxidative parameters in patients with spinal cord injury: implications in the pathogenesis of disease. Spinal Cord 53:3-6.
Fleming JC, Norenberg MD, Ramsay DA, Dekaban GA, Marcillo AE, Saenz AD, Pasquale-Styles M, Dietrich WD, Weaver LC (2006) The cellular inflammatory response in human spinal cords after injury. Brain 129:3249-3269.
Forghani R, Wojtkiewicz GR, Zhang Y, Seeburg D, Bautz BR, Pulli B, Milewski AR, Atkinson WL, Iwamoto Y, Zhang ER, Etzrodt M, Rodriguez E, Robbins CS, Swirski FK, Weissleder R, Chen JW (2012) Demyelinating diseases: myeloperoxidase as an imaging biomarker and therapeutic target. Radiology 263:451-460.
Franceschini A, Szklarczyk D, Frankild S, Kuhn M, Simonovic M, Roth A, Lin J, Minguez P, Bork P, von Mering C, Jensen LJ (2013) STRING v9.1: protein-protein interaction networks, with increased coverage and integration. Nucleic Acids Res 41:D808-815.
Fujino T, Watanabe K, Beppu M, Kikugawa K, Yasuda H (2000) Identification of oxidized protein hydrolase of human erythrocytes as acylpeptide hydrolase. Biochim Biophys Acta 1478:102-112.
Gorudko IV, Sokolov AV, Shamova EV, Grigorieva DV, Mironova EV, Kudryavtsev IV, Gusev SA, Gusev AA, Chekanov AV, Vasilyev VB, Cherenkevich SN, Panasenko OM, Timoshenko AV (2016) Binding of human myeloperoxidase to red blood cells: Molecular targets and biophysical consequences at the plasma membrane level. Arch Biochem Biophys 591:87-97.
Guest PC, Gottschalk MG, Bahn S (2013) Proteomics: improving biomarker translation to modern medicine? Genome Med 5:17.
Hall ED (2011) Antioxidant therapies for acute spinal cord injury. Neurotherapeutics 8:152-167.
Hayes JD, Flanagan JU, Jowsey IR (2005) Glutathione transferases. Annu Rev Pharmacol Toxicol 45:51-88.
Jansen E, Beekhof PK, Viezeliene D, Muzakova V, Skalicky J (2017) Long-term stability of oxidative stress biomarkers in human serum. Free Radic Res 51:970-977.

Jeffery ND, Lakatos A, Franklin RJ (2005) Autologous olfactory glial cell transplantation is reliable and safe in naturally occurring canine spinal cord injury. J Neurotrauma 22:1282-1293.
Jia Z, Zhu H, Li J, Wang X, Misra H, Li Y (2012) Oxidative stress in spinal cord injury and antioxidant-based intervention. Spinal Cord 50:264-274.
Kamencic H, Griebel RW, Lyon AW, Paterson PG, Juurlink BH (2001) Promoting glutathione synthesis after spinal cord trauma decreases secondary damage and promotes retention of function. FASEB J 15:243-250.
Keeney JT, Swomley AM, Förster S, Harris JL, Sultana R, Butterfield DA (2013) Apolipoprotein A-I: insights from redox proteomics for its role in neurodegeneration. Proteomics Clin Appl 7:109-122.
Khoubnasabjafari M, Ansarin K, Jouyban A (2015) Reliability of malondialdehyde as a biomarker of oxidative stress in psychological disorders. Bioimpacts 5:123-127.
Kubota K, Saiwai H, Kumamaru H, Maeda T, Ohkawa Y, Aratani Y, Nagano T, Iwamoto Y, Okada S (2012) Myeloperoxidase exacerbates secondary injury by generating highly reactive oxygen species and mediating neutrophil recruitment in experimental spinal cord injury. Spine (Phila Pa 1976) 37:1363-1369.
Kumar A, Dhull DK, Gupta V, Channana P, Singh A, Bhardwaj M, Ruhal P, Mittal R (2017) Role of Glutathione-S-transferases in neurological problems. Expert Opin Ther Pat 27:299-309.
Lassmann H, van Horssen J (2016) Oxidative stress and its impact on neurons and glia in multiple sclerosis lesions. Biochim Biophys Acta 1862:506-510.
Lefkowitz DL, Lefkowitz SS (2008) Microglia and myeloperoxidase: a deadly partnership in neurodegenerative disease. Free Radic Biol Med 45:726-731.
Lucantoni G, Pietraforte D, Matarrese P, Gambardella L, Metere A, Paone G, Bianchi EL, Straface E (2006) The red blood cell as a biosensor for monitoring oxidative imbalance in chronic obstructive pulmonary disease: an ex vivo and in vitro study. Antioxid Redox Signal 8:1171-1182.
Mazzulla S, Schella A, Gabriele D, Baldino N, Sesti S, Perrotta E, Costabile A, de Cindio B (2015) Oxidation of human red blood cells by a free radical initiator: effects on rheological properties. Clin Hemorheol Microcirc 60:375-388.
Meloni L, Manca MR, Loddo I, Cioglia G, Cocco P, Schwartz A, Muntoni S, Muntoni S (2008) Glucose-6-phosphate dehydrogenase deficiency protects against coronary heart disease. J Inherit Metab Dis 31:412-417.
Michalski A, Damoc E, Hauschild JP, Lange O, Wieghaus A, Makarov A, Nagaraj N, Cox J, Mann M, Horning S (2011) Mass spectrometry-based proteomics using Q Exactive, a high-performance benchtop quadrupole Orbitrap mass spectrometer. Mol Cell Proteomics 10:M111.011015.
Moore SA, Granger N, Olby NJ, Spitzbarth I, Jeffery ND, Tipold A, Nout-Lomas YS, da Costa RC, Stein VM, Noble-Haeusslein LJ, Blight AR, Grossman RG, Basso DM, Levine JM (2017) Targeting translational successes through CANSORT-SCI: using pet dogs to identify effective treatments for spinal cord injury. J Neurotrauma 34:2007-2018.
Motiei-Langroudi R, Sadeghian H (2017) Traumatic spinal cord injury: long-term motor, sensory, and urinary outcomes. Asian Spine J 11:412-418.
Myers J, Lee M, Kiratli J (2007) Cardiovascular disease in spinal cord injury: an overview of prevalence, risk, evaluation, and management. Am J Phys Med Rehabil 86:142-152.
Nightingale TE, Bhangu GS, Bilzon JLJ, Krassioukov AV (2020) A cross-sectional comparison between cardiorespiratory fitness, level of lesion and red blood cell distribution width in adults with chronic spinal cord injury. J Sci Med Sport 23:106-111.
Odobasic D, Kitching AR, Holdsworth SR (2016) Neutrophil-mediated regulation of innate and adaptive immunity: the role of myeloperoxidase. J Immunol Res 2016:2349817.
Ogasawara Y, Funakoshi M, Ishii K (2008) Pyruvate kinase is protected by glutathione-dependent redox balance in human red blood cells exposed to reactive oxygen species. Biol Pharm Bull 31:1875-1881.
Okamoto K, Maruyama T, Kaji Y, Harada M, Mawatari S, Fujino T, Uyesaka N (2004) Verapamil prevents impairment in filterability of human erythrocytes exposed to oxidative stress. Jpn J Physiol 54:39-46.
Ozgurtas T, Alaca R, Gulec M, Kutluay T (2003) Do spinal cord injuries adversely affect serum lipoprotein profiles? Mil Med 168:545-547.
Pallotta V, Rinalducci S, Zolla L (2015) Red blood cell storage affects the stability of cytosolic native protein complexes. Transfusion 55:1927-1936.
Pandey KB, Rizvi SI (2011) Biomarkers of oxidative stress in red blood cells. Biomed Pap Med Fac Univ Palacky Olomouc Czech Repub 155:131-136.
Parent BA, Seaton M, Sood RF, Gu H, Djukovic D, Raftery D, O'Keefe GE (2016) Use of metabolomics to trend recovery and therapy after injury in critically ill trauma patients. JAMA Surg 151:e160853.
Pasini EM, Kirkegaard M, Mortensen P, Lutz HU, Thomas AW, Mann M (2006) In-depth analysis of the membrane and cytosolic proteome of red blood cells. Blood 108:791-801.
Perl A, Hanczko R, Telarico T, Oaks Z, Landas S (2011) Oxidative stress, inflammation and carcinogenesis are controlled through the pentose phosphate pathway by transaldolase. Trends Mol Med 17:395-403.
Phillips AA, Krassioukov AV (2015) Contemporary cardiovascular concerns after spinal cord injury: mechanisms, maladaptations, and management. J Neurotrauma 32:1927-1942.
Revin VV, Gromova NV, Revina ES, Samonova AY, Tychkov AY, Bochkareva SS, Moskovkin AA, Kuzmenko TP (2019) The influence of oxidative stress and natural antioxidants on morphometric parameters of red blood cells, the hemoglobin oxygen binding capacity, and the activity of antioxidant enzymes. Biomed Res Int 2019:2109269.
Rinaldi C, Bramanti P, Famà A, Scimone C, Donato L, Antognelli C, Alafaci C, Tomasello F, D'Angelo R, Sidoti A (2015) Glyoxalase I A111E, Paraoxonase 1 Q192R and L55M Polymorphisms in Italian patients with sporadic cerebral cavernous malformations: a pilot study. J Biol Regul Homeost Agents 29:493-500.
Rios C, Santander I, Méndez-Armenta M, Nava-Ruiz C, Orozco-Suárez S, Islas M, Barón-Flores V, Diaz-Ruiz A (2018) Metallothionein-I+II reduces oxidative damage and apoptosis after traumatic spinal cord injury in rats. Oxid Med Cell Longev 2018:3265918.
Rokicki W, Zalejska-Fiolka J, Pojda-Wilczek D, Kabiesz A, Majewski W (2016) Oxidative stress in the red blood cells of patients with primary open-angle glaucoma. Clin Hemorheol Microcirc 62:369-378.
Ryu HH, Lim JH, Byeon YE, Park JR, Seo MS, Lee YW, Kim WH, Kang KS, Kweon OK (2009) Functional recovery and neural differentiation after transplantation of allogenic adipose-derived stem cells in a canine model of acute spinal cord injury. J Vet Sci 10:273-284.
Scheltema RA, Hauschild JP, Lange O, Hornburg D, Denisov E, Damoc E, Kuehn A, Makarov A, Mann M (2014) The Q Exactive HF, a Benchtop mass spectrometer with a pre-filter, high-performance quadrupole and an ultra-high-field Orbitrap analyzer. Mol Cell Proteomics 13:3698-3708.
Sharma R, Yang Y, Sharma A, Awasthi S, Awasthi YC (2004) Antioxidant role of glutathione S-transferases: protection against oxidant toxicity and regulation of stress-mediated apoptosis. Antioxid Redox Signal 6:289-300.
Tang HY, Ho HY, Wu PR, Chen SH, Kuypers FA, Cheng ML, Chiu DT (2015) Inability to maintain GSH pool in G6PD-deficient red cells causes futile AMPK activation and irreversible metabolic disturbance. Antioxid Redox Signal 22:744-759.
Tavora FR, Ripple M, Li L, Burke AP (2009) Monocytes and neutrophils expressing myeloperoxidase occur in fibrous caps and thrombi in unstable coronary plaques. BMC Cardiovasc Disord 9:27.
Tsakanova G, Arakelova E, Ayvazyan V, Ayvazyan A, Tatikyan S, Aroutiounian R, Dalyan Y, Haroutiunian S, Tsakanov V, Arakelyan A (2017) Two-photon microscopy imaging of oxidative stress in human living erythrocytes. Biomed Opt Express 8:5834-5846.
Tully M, Zheng L, Shi R (2014) Acrolein detection: potential theranostic utility in multiple sclerosis and spinal cord injury. Expert Rev Neurother 14:679-685.
Visavadiya NP, Patel SP, VanRooyen JL, Sullivan PG, Rabchevsky AG (2016) Cellular and subcellular oxidative stress parameters following severe spinal cord injury. Redox Biol 8:59-67.
Walldius G, Jungner I, Holme I, Aastveit AH, Kolar W, Steiner E (2001) High apolipoprotein B, low apolipoprotein A-I, and improvement in the prediction of fatal myocardial infarction (AMORIS study): a prospective study. Lancet 358:2026-2033.
Woźniak B, Woźniak A, Mila-Kierzenkowska C, Kasprzak HA (2016) Correlation of oxidative and antioxidative processes in the blood of patients with cervical spinal cord injury. Oxid Med Cell Longev 2016:6094631.
Xu BP, Yao M, Li ZJ, Tian ZR, Ye J, Wang YJ, Cui XJ (2020) Neurological recovery and antioxidant effects of resveratrol in rats with spinal cord injury: a meta-analysis. Neural Regen Res 15:482-490.
Xu W, Chi L, Xu R, Ke Y, Luo C, Cai J, Qiu M, Gozal D, Liu R (2005) Increased production of reactive oxygen species contributes to motor neuron death in a compression mouse model of spinal cord injury. Spinal Cord 43:204-213.
Yao X, Zhang Y, Hao J, Duan HQ, Zhao CX, Sun C, Li B, Fan BY, Wang X, Li WX, Fu XH, Hu Y, Liu C, Kong XH, Feng SQ (2019) Deferoxamine promotes recovery of traumatic spinal cord injury by inhibiting ferroptosis. Neural Regen Res 14:532-541.
Yap YW, Whiteman M, Bay BH, Li Y, Sheu FS, Qi RZ, Tan CH, Cheung NS (2006) Hypochlorous acid induces apoptosis of cultured cortical neurons through activation of calpains and rupture of lysosomes. J Neurochem 98:1597-1609.
Zhang L, Zhuang X, Chen Y, Niu Z, Xia H (2020) Plasma erythropoietin, IL-17A, and IFNγ as potential biomarkers of motor function recovery in a canine model of spinal cord injury. J Mol Neurosci doi: 10.1007/s12031-020-01575-y.

P-Reviewers: Ryu JK, Rodemer WS; C-Editor: Zhao M; S-Editors: Kreiner L, Yu J, Li CH; L-Editors: Yu J, Song LP; T-Editor: Jia Y

Additional Table 1 Gene ontology (GO) functional enrichment analysis for the differentially expressed proteins in erythrocytes of dogs following spinal cord injury

Term	Category	*P*-value	UniProt ID
Biological process			
Cell migration	GO:0016477	2.25E-06	F1Q421, F1PBI6, F1PDJ5, E2QWN7, E2QSZ5, Q8MJD1
Cell motility	GO:0048870	3.44E-06	F1Q421, F1PBI6, F1PDJ5, E2QWN7, E2QSZ5, Q8MJD1
Localization of cell	GO:0051674	3.44E-06	F1Q421, F1PBI6, F1PDJ5, E2QWN7, E2QSZ5, Q8MJD1
Locomotion	GO:0040011	8.31E-06	F1Q421, F1PBI6, F1PDJ5, E2QWN7, E2QSZ5, Q8MJD1
Movement of cell or subcellular component	GO:0006928	1.22E-05	F1Q421, F1PBI6, F1PDJ5, E2QWN7, E2QSZ5, Q8MJD1
Phagocytosis	GO:0006909	2.65E-05	E2QSZ5, Q8MJD1, F1PBI6
Fibrinolysis	GO:0042730	5.62E-05	F1Q421, F1PBI6
Immune response	GO:0006955	6.72E-05	E2QSZ5, E2QWN7, Q8MJD1, F1PDJ5, F1PBI6
Response to stress	GO:0006950	7.04E-05	F1Q421, F1PBI6, E2QWE0, F1PDJ5, Q8MJD1, E2QSZ5, J9P0R6
Negative regulation of cytokine production	GO:0001818	7.37E-05	Q8MJD, F1PDJ5, F1PBI6
Negative regulation of response to external stimulus	GO:0032102	8.06E-05	F1Q421, F1PDJ5, F1PBI6
Immune system process	GO:0002376	8.48E-05	F1Q421, F1PBI6, F1PDJ5, E2QWN7, E2QSZ5, Q8MJD1
Defense response	GO:0006952	9.91E-05	J9P0R6, E2QSZ5, Q8MJD1, F1PDJ5, F1PBI6
Cell-substrate adhesion	GO:0031589	1.12E-04	E2QSZ5, F1PBI6, F1PDJ5
Immune effector process	GO:0002252	1.14E-04	E2QSZ5, E2QWN7, Q8MJD1, F1PDJ5
Molecular function			
Lipoprotein particle receptor binding	GO:0070325	1.31E-02	F1PDJ5
Protein-lipid complex binding	GO:0071814	5.62E-05	F1PBI6, F1PDJ5
Sulfur compound binding	GO:1901681	7.71E-05	F1Q2D2, Q8MJD1, F1PBI6
Modified amino acid binding	GO:0072341	2.11E-04	F1Q2D2, F1PBI6
Macromolecular complex binding	GO:0044877	7.17E-04	E2QSZ5, E2QWN7, F1PBI6, F1PDJ5
Identical protein binding	GO:0042802	8.79E-04	E2QSZ5, E2QWN7, F1Q2D2, F1PDJ5
Actin filament binding	GO:0051015	1.13E-03	E2QSZ5, E2QWN7
Protein complex binding	GO:0032403	1.53E-03	E2QSZ5, E2QWN7, F1PBI6
Heparin binding	GO:0008201	1.64E-03	Q8MJD1, F1PBI6
Serine-type endopeptidase activity	GO:0004252	2.75E-03	F1Q421, Q8MJD1
Glycosaminoglycan binding	GO:0005539	2.84E-03	Q8MJD1, F1PBI6
Peptide binding	GO:0042277	3.41E-03	F1Q2D2, F1PDJ5
Peptidase activity	GO:0008233	3.43E-03	E2QWE0, F1Q421, Q8MJD1
Serine-type peptidase activity	GO:0008236	3.61E-03	F1Q421, Q8MJD1
Amide activity	GO:0033218	3.81E-03	F1Q2D2, F1PDJ5
Cellular component			
Cytoplasmic, membrane-bounded vesicle	GO:0016023	9.07E-06	E2QWE0, E2QSZ5, Q8MJD1, F1PDJ5, F1PBI6
Cytoplasmic vesicle	GO:0031410	1.63E-05	E2QWE0, E2QSZ5, Q8MJD1, F1PDJ5, F1PBI6
Intracellular vesicle	GO:0097708	1.66E-05	E2QWE0, E2QSZ5, Q8MJD1, F1PDJ5, F1PBI6
Phagocytic cup	GO:0001891	5.62E-05	E2QSZ5, E2QWN7
Membrane-bounded vesicle	GO:0031988	1.20E-04	F1PDJ5, F1PBI6, E2QWE0, F1Q2D2, E2QWN7, E2QSZ5, Q8MJD1
Vesicle	GO:0031982	1.51E-04	F1PDJ5, F1PBI6, E2QWE0, F1Q2D2, E2QWN7, E2QSZ5, Q8MJD1
Secretory vesicle	GO:0099503	3.55E-04	E2QWE0, Q8MJD1, F1PBI6

Actin filament	GO:0005884	4.26E-04	E2QSZ5, E2QWN7
Extracellular exosome	GO:0070062	4.34E-04	F1PDJ5, F1PBI6, F1Q2D2, E2QWN7, E2QSZ5, Q8MJD1
Extracellular organelle	GO:0043230	4.47E-04	F1PDJ5, F1PBI6, F1Q2D2, E2QWN7, E2QSZ5, Q8MJD1
Extracellular vesicle	GO:1903561	4.47E-04	F1PDJ5, F1PBI6, F1Q2D2, E2QWN7, E2QSZ5, Q8MJD1
Endocytic vesicle	GO:0030139	1.64E-03	E2QSZ5, F1PDJ5
Extracellular region	GO:0005576	7.51E-04	F1PDJ5, F1PBI6, F1Q2D2, E2QWN7, E2QSZ5, Q8MJD1, F1Q421
Extracellular space	GO:0005615	1.86E-03	E2QWN7, Q8MJD1, F1PDJ5, F1PBI6
Extracellular region part	GO:0044421	3.09E-03	F1PDJ5, F1PBI6, F1Q2D2, E2QWN7, E2QSZ5, Q8MJD1

Category refers to the GO functional categories.

Additional Table 2 Pathway enrichment analysis for the differentially expressed proteins in erythrocytes following spinal cord injury

Term	Category	*P*-value	UniProt ID
Phagosome	cfa04145	0.0002	E2QSZ5, J9P0R6, F1PBI6
Glutathione metabolism	cfa00480	0.0008	F1Q0J0, F1Q2D2
Transcriptional misregulation in cancer	cfa05202	0.0050	Q8MJD1, J9P0R6
Metabolic pathways	cfa01100	0.1977	F1Q2D2, H9GW87
Vitamin digestion and absorption	cfa04977	0.0208	F1PDJ5
Pentose phosphate pathway	cfa00030	0.0233	H9GW87
Cysteine and methionine metabolism	cfa00270	0.0259	F1Q2D2
Fat digestion and absorption	cfa04975	0.0298	F1PDJ5
Bladder cancer	cfa05219	0.0361	F1PBI6
Staphylococcus aureus infection	cfa05150	0.0374	F1Q421
African trypanosomiasis	cfa05143	0.0425	F1PDJ5
Biosynthesis of amino acids	cfa01230	0.0475	H9GW87
Drug metabolism - cytochrome P450	cfa00982	0.0488	F1Q0J0
Metabolism of xenobiotics by cytochrome P450	cfa00980	0.0500	F1Q0J0
Extracellular matrix-receptor interaction	cfa04512	0.0538	F1PBI6

Category refers to the pathway functional categories.